Supplementary Materials

Non-resonant Plasmon Energy Transfer Processes for Catalysis

Arthur Andreis [1]*, Jorge Herrera[2], Virginie Mouriès-Mansuy[2], Cyril Ollivier[2], Salem Ba Sowid[3], François Ribot[4], Louis Fensterbank[2,3]*, Jacinto Sá[1,5]*

[1] Department of Chemistry-Ångström, Uppsala University; Uppsala, 751 20, Sweden.

[2] Institut Parisien de Chimie Moléculaire, Sorbonne Université, CNRS; Paris, F-75005, France.

[3] Collège de France, CNRS, Sorbonne Université, Laboratoire d'Activation Moléculaire, 11 place Marcelin Berthelot, F-75005 Paris, France.

[4] Laboratoire de Chimie de la Matie re Condensée de Paris (LCMCP), Sorbonne Université, CNRS, F-75252 Paris Cedex 05, France.

[5] Institute of Physical Chemistry, Polish Academy of Sciences; Warsaw, 01-224, Poland.

* louis.fensterbank@college-de-france.fr; jacinto.sa@kemi.uu.se

Materials and Methods

Reagents/Solvents

Tannic acid ($Na_3C_6H_5O_7$), sodium citrate tribasic dihydrate ($Na_3C_6H_5O_7{\cdot}2H_2O$), hydrogen tetrachloroaurate (III) ($HAuCl_4$), 1-naphthoic acid ($C_{11}H_8O_2$; NCA) and (*p*-$CF_3Ph)_3PAuCl$ were acquired in high purity from Sigma-Aldrich. Anhydrous K_2CO_3 was purchased from Alfa Aesar. $Ir[dF(CF_3)ppy]_2(dtbbpy)PF_6$ [(**Ir-F**)] was purchased from BLD-pharm.

2-(*p*-Tolylethynyl)phenol was synthesized following the previous reported procedure.[1a] Acetonitrile (MeCN) was obtained free of water and kept under argon atmosphere using a Solvent Purification System (SPS) (PureSolv MD 5). Milli-Q water was obtained from a Milli-DI® System. Argon and Air gases used for purging the solution were obtained in high purity from Air Liquid.

Synthesis of Au-complex [(**Au-CF$_3$**)]

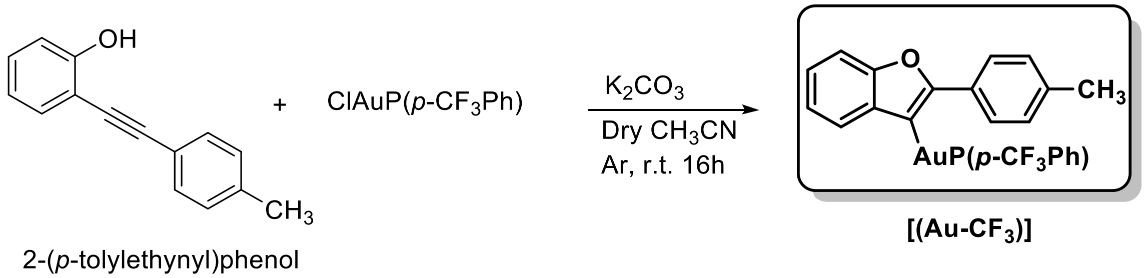

(2-(*p*-Tolyl)benzofuranyl)((tri(*p*-trifluomethyl)phenylphosphine)gold was synthesized as previously reported[1a,b] starting from 2-(phenylethynyl)phenol instead of methyl-*N*-(2-(*p*-tolylethynyl)phenyl)benzenesulfonamide. In a 25-mL Schlenk tube, 120 mg (171.9 µmol, 1 eq.) of (*p*-$CF_3Ph)_3PAuCl$, 35.8 mg (171.9 µmol, 1 eq.) of 2-(phenylethynyl)phenol **3a**, and 59.4 mg (429.8 µmol, 2.5 eq.) of K_2CO_3 were dissolved in 7 mL of dry acetonitrile and stirred for 16 h at r.t. covered with aluminium foil from the light. The mixture was filtered over a small column of basic aluminum oxide and washed with 50 mL of dry acetonitrile. The solvent was removed in the rotary evaporator without heating, giving [(Au-CF_3)] as white solid, 136.4 mg, 91.2%.

Spectral data are in accordance with those reported in the literature in CD_3CN (*36a*). ^1H NMR (300 MHz, CD_2Cl_2) δ 8.29 (d, J = 6 Hz, 2H), 7.87-7.76 (m, 13 H), 7.49 (d, J = 6 Hz, 1H), 7.20-7.14 (m, 4H), 2.39 (s, 3H) ppm. ^{19}F NMR (282 MHz, CD_2Cl_2) δ -63.52 ppm. ^{31}P NMR (122 MHz, CD_2Cl_2) δ 45.70 ppm.

Gold nanoparticles synthesis

To synthesize the gold nanoparticles used in this study (AuNP) in water, a modified version of the Turkevich method was employed.[2] The method employs hydrogen tetrachloroaurate (III) as the gold precursor, tannic acid to adjust the solution's pH, and sodium citrate as both the reducing agent and stabilizer.

In a 100 mL round-bottom flask, 50 mL of an aqueous solution containing 97.0 mg (0.33 mmol; 6.60 mM; 13 200 equiv.) of sodium citrate dihydrate and 212.65 mg (0.13 mmol; 2.5 mM; 5000 equiv) of tannic acid were stirred in an oil bath at 70 °C for 10 min. Then, 4.25 mg (25 nmol; 0.5 μM; 1 equiv.) of a solution of 25 mM $HAuCl_4$ (1 mL) was rapidly added to the mixture and the suspension was stirred for additional 5 min, resulting in an abrupt change of color from light yellow to deep red. The mixture was then protected from light, cooled to room temperature and then stored in the fridge at 4 °C. If there was decantation of the AuNP after 4 days, the yellow supernatant was removed, and 60 mL water was added to resuspend the nanoparticles in water and reduce the salt concentration.

Gold phase transfer to acetonitrile

High salt concentration can significantly hinder the phase transfer of AuNPs from water to organic solvents. To address this, the initial step of the transfer process focused on reducing the salt content in the aqueous AuNP suspension, following a procedure adapted from the literature.[3] Briefly, 2 mL Eppendorfs (10 per batch) containing 1 mL AuNP each (10 mL) were centrifuged (12000 rpm, 5 min), the supernatant was removed (around 15 μL of the aqueous suspension remained), and water was carefully added to avoid resuspension of the nanoparticles. After 10 min, the process was repeated without the centrifugation step. This washing cycle was performed up to 2 times, after which the supernatant was removed and acetonitrile (MeCN) was added to resuspend the suspension (typically 1 mL was used to mix 5 Eppendorfs). The 2 remaining Eppendorfs (2 mL) were then centrifuged (12000 rpm, 5 min), the supernatant was removed and MeCN was added so that the final concentration of water in the mixture was less than 0.2% (v/v).

AuNP functionalization

To functionalize the AuNPs with NCA in MeCN, a 40 mM NCA solution was pre-prepared in MeCN. Afterwards, in a 4 mL vial, NCA, AuNP and MeCN were added so that the final concentration of NCA was 20 mM and AuNP had an A = 0.6 at λ_{max} = 540 nm. NCA and MeCN were added first to avoid high concentrations of NCA, and then the AuNP as this seems to prevent nanoparticles aggregation. The purple suspension was shaken gently for 20 s and allowed to rest at room temperature, protected from light for 24 h. After that period, the suspension was stored at 4 °C until further use.

AuNP size determination

The nanoparticles' size was assessed using Dynamic Light Scattering (DLS) in a Quartz cuvette (3 mL; samples in MeCN) or a disposable cuvette (1.5 mL; samples in H_2O). The measurements were complemented with Transmission Electron Microscopy (TEM). TEM sample was prepared by dropping a diluted AuNPs suspension onto a copper grid coated with a carbon film and allowing the water to evaporate in air. The TEM images were obtained using a Tecnai Spirit G2 microscope operating at 120 kV. The size distribution histogram and average size were obtained by manually measuring at least 400 particles using the ImageJ software.

Raman spectroscopy

Raman spectroscopy measurements were carried out using an inVia confocal Raman microscope with 532 nm laser excitation and a 20× objective lens. All samples were analyzed in solution.

UV-Vis spectroscopy and Photoluminescence

Samples were analyzed using a Cary 60 Spectrophotometer (Agilent; Absorption) and a FS5 Spectrofluorimeter (Edinburgh Instruments; Photoluminescence). The spectra were recorded in the 200-800 nm range and a standard Quartz cuvette (3 mL) was used. For the Stern-Volmer plot, the emitter (NCA) and the quencher (Au-CF_3) showed less emission alone than mixed. For this reason, the solution with the smallest quencher concentration ($1,4 \times 10^{-4}$ mol × L^{-1}) was chosen as the first point of the curve following an adapted version of the Stern-Volmer equation:

$$\frac{I_0}{I} = K_{SV} \times [Au - CF_3] \qquad \text{(eq. S1)}$$

Where:

I_0 = Intensity of fluorescence at smallest concentration of quencher

I = Intensity of fluorescence

K_{SV} = Stern-Volmer constant

After the fitting, the following equation was obtained:

$$\frac{I_0}{I} = 0{,}25242 + 4{,}8 \times 10^3 \times [Au - CF_3] \quad \text{(eq. S2)}$$

So K_{SV} = 4,8 × 10^{-3} M^{-1}

Fourier-Transformed Infrared (FT-IR) spectroscopy

FT-IR spectra were recorded in a Vertex V-70 (Bruker) using the transmission mode. The spectra were recorded in the 700-4000 cm^{-1} range using a Micro Compression Cell (Specac) and 80 μL of sample per measurement.

Flash photolysis transient absorption spectroscopy (TAS)

Spectra were recorded in the 1-10000 ns time range and 330-730 nm range using pump-probe spectroscopy in a Quartz cuvette (3 mL). The source of the pump was an EKSPLA NT242 and the probe source was a LP920 (Edinburgh Instruments). For experiments under Ar, samples in the cuvette were initially bubbled with Ar for at least 10 min, then closed with a lid and measured instantly. For experiments identified as "O_2", the sample was measured without addition of Ar or air was bubbled in the sample if Ar had been previously added.

The decay of the light absorbers was fitted with a single exponential. Considering that the formation of the Au-CF_3 $^3MLCT_1$ state (i.e. Au-CF_3^3) resembles the formation of an intermediate, the model equation for consecutive reactions was used to fit the curve of Au-CF_3^3:

$$[Au - CF_3]^3 = \frac{k_1 \times [Ir]_0}{k_2 - k_1} \times (e^{-k_1 t} - e^{-k_2 t}) + c \qquad \text{(eq. S3)}$$

Where:

k_1 = Formation constant of Au-CF_3^3

k_2 = Decay constant of Au-CF_3^3

c = Constant

$[Au - CF_3]^3$ = Concentration of Au-CF_3^3

$[Ir]_0$ = Initial concentration of Ir-F photocatalyst

Supporting data

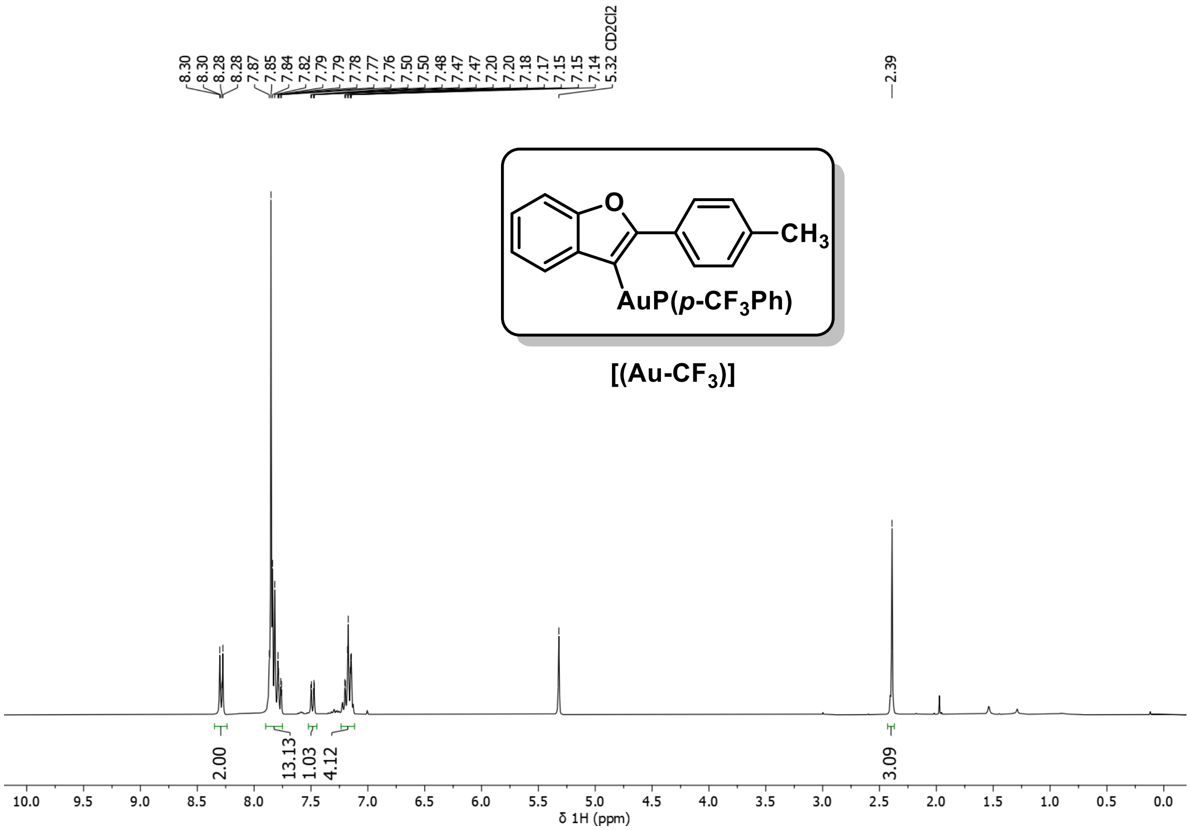

Fig. S1. ^{1}H-NMR 300 MHz of Au-CF$_3$ in CD$_2$Cl$_2$.

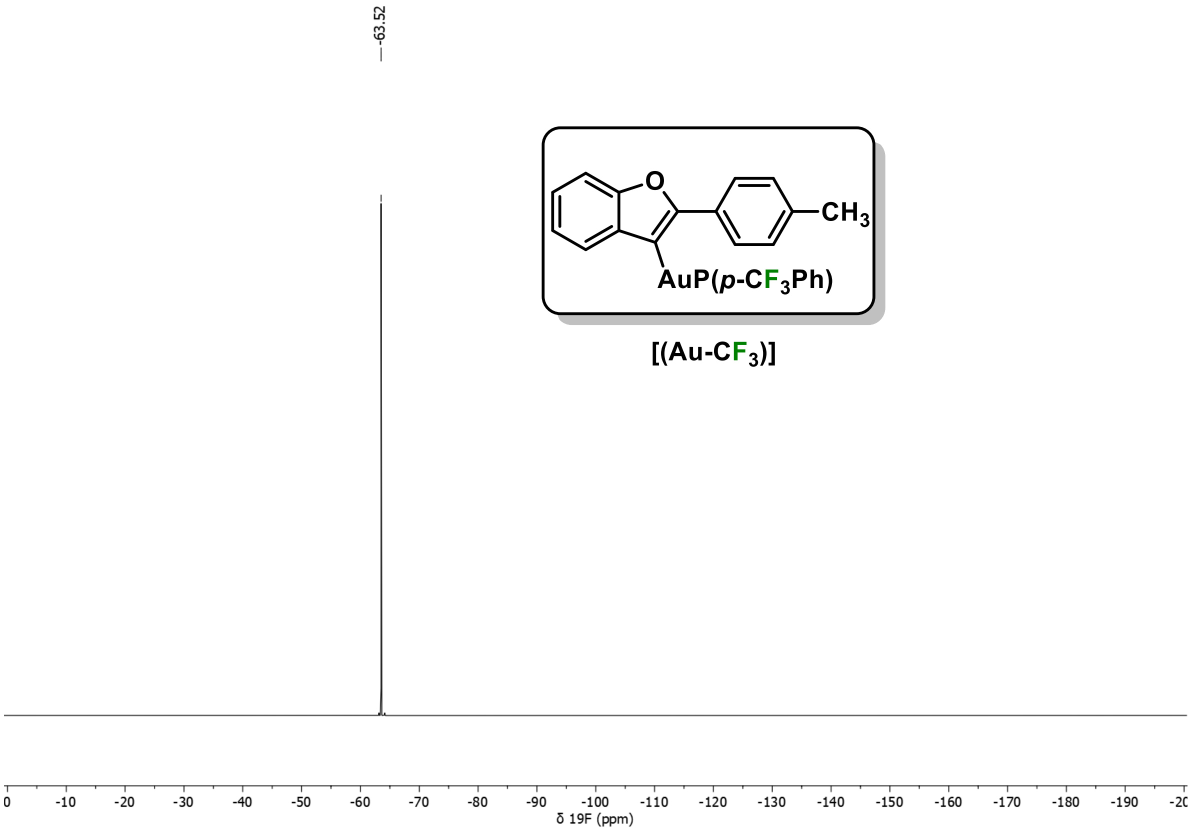

Fig. S2. ^{19}F-NMR 282 MHz of Au-CF$_3$ in CD$_2$Cl$_2$.

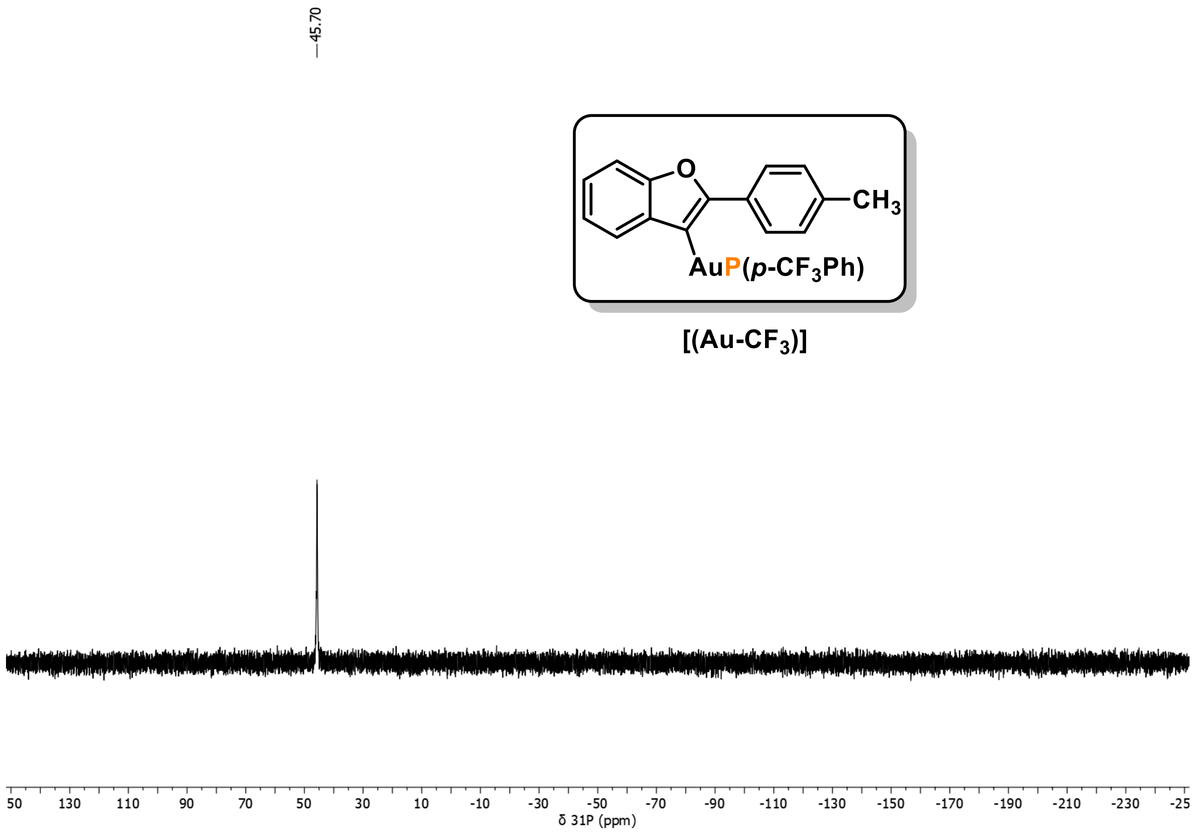

Fig. S3. ^{31}P-NMR 122 MHz of Au-CF$_3$ in CD$_2$Cl$_2$.

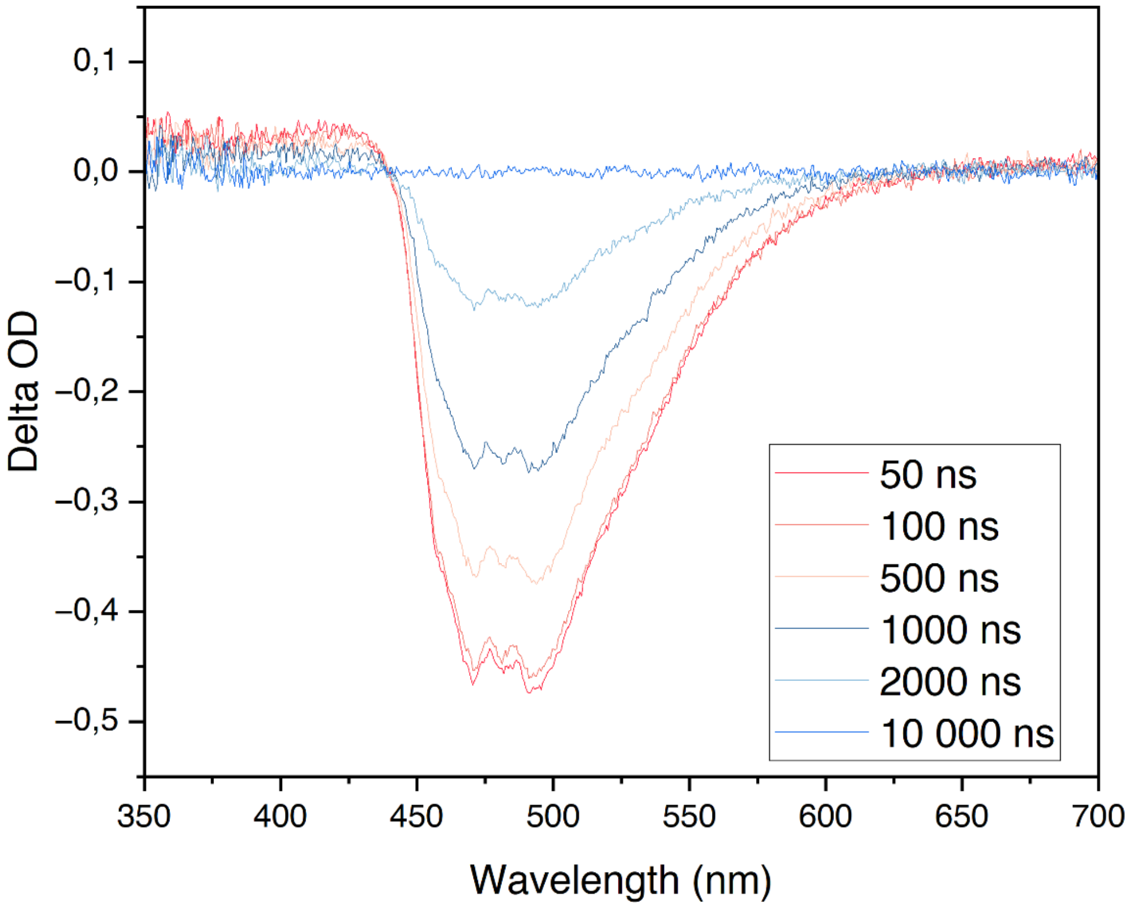

Fig. S4. Transient spectral changes of Ir-F photosensitizer after excitation at 410 nm.

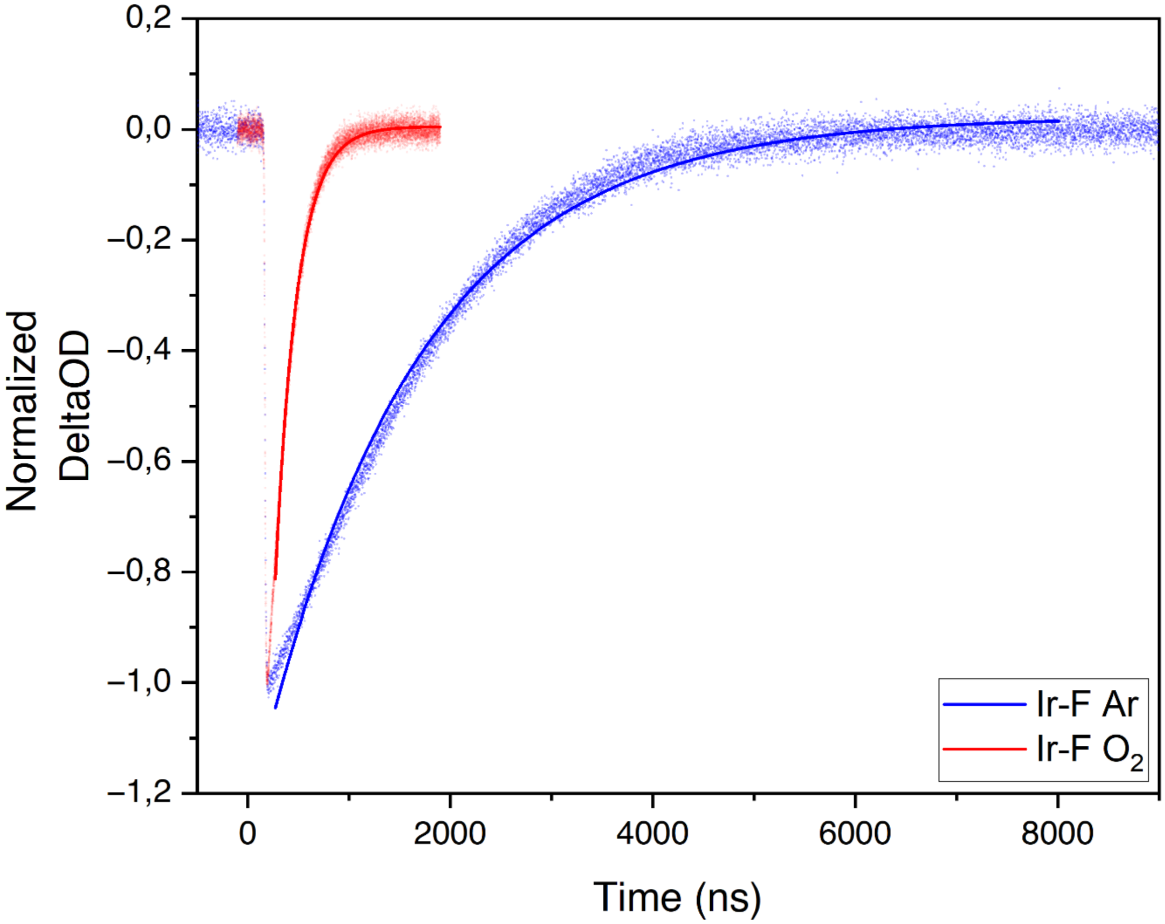

Fig. S5. Kinetic traces extracted at 490 nm, minimum of the TAS signal from Fig. S1, after excitation of the Ir-F photosensitizer at 410 nm. The graph compares the signal decay in inert gas (Argon) and in the presence of oxygen.

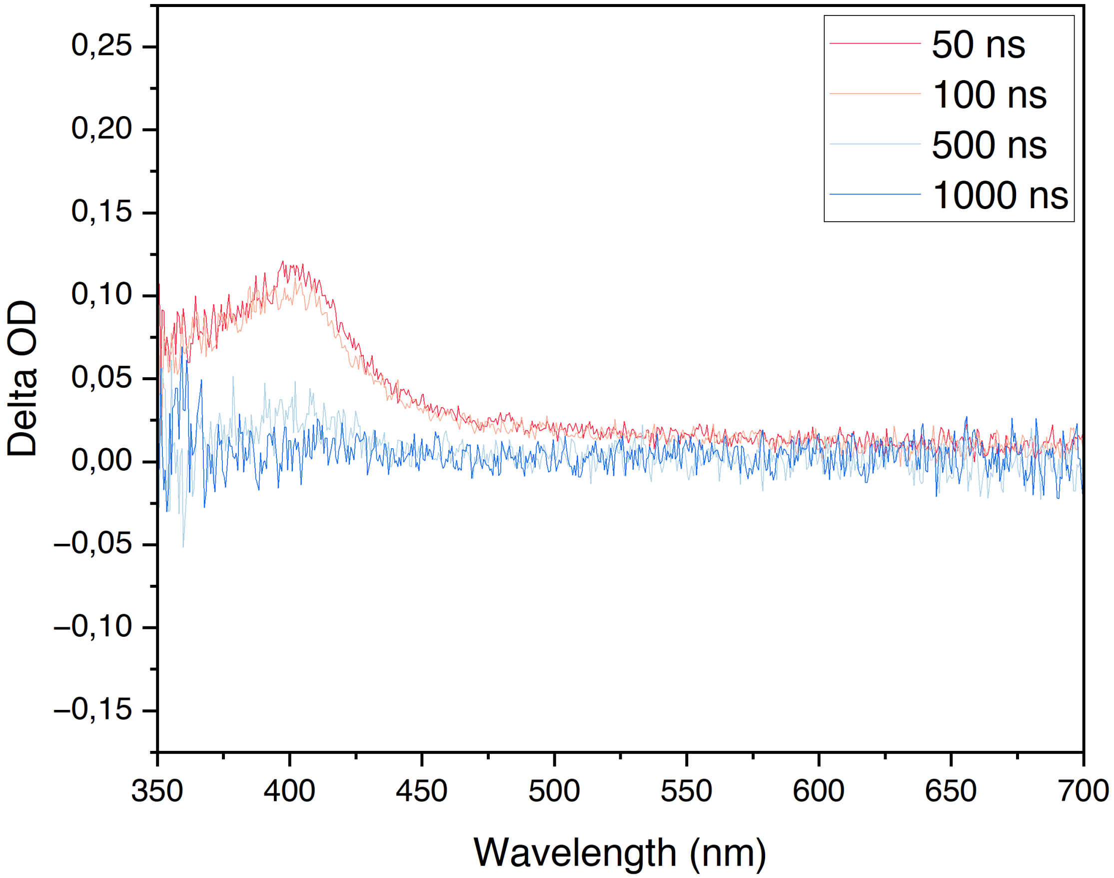

Fig. S6. Transient spectral changes of Au-CF$_3$ complex after excitation at 355 nm.

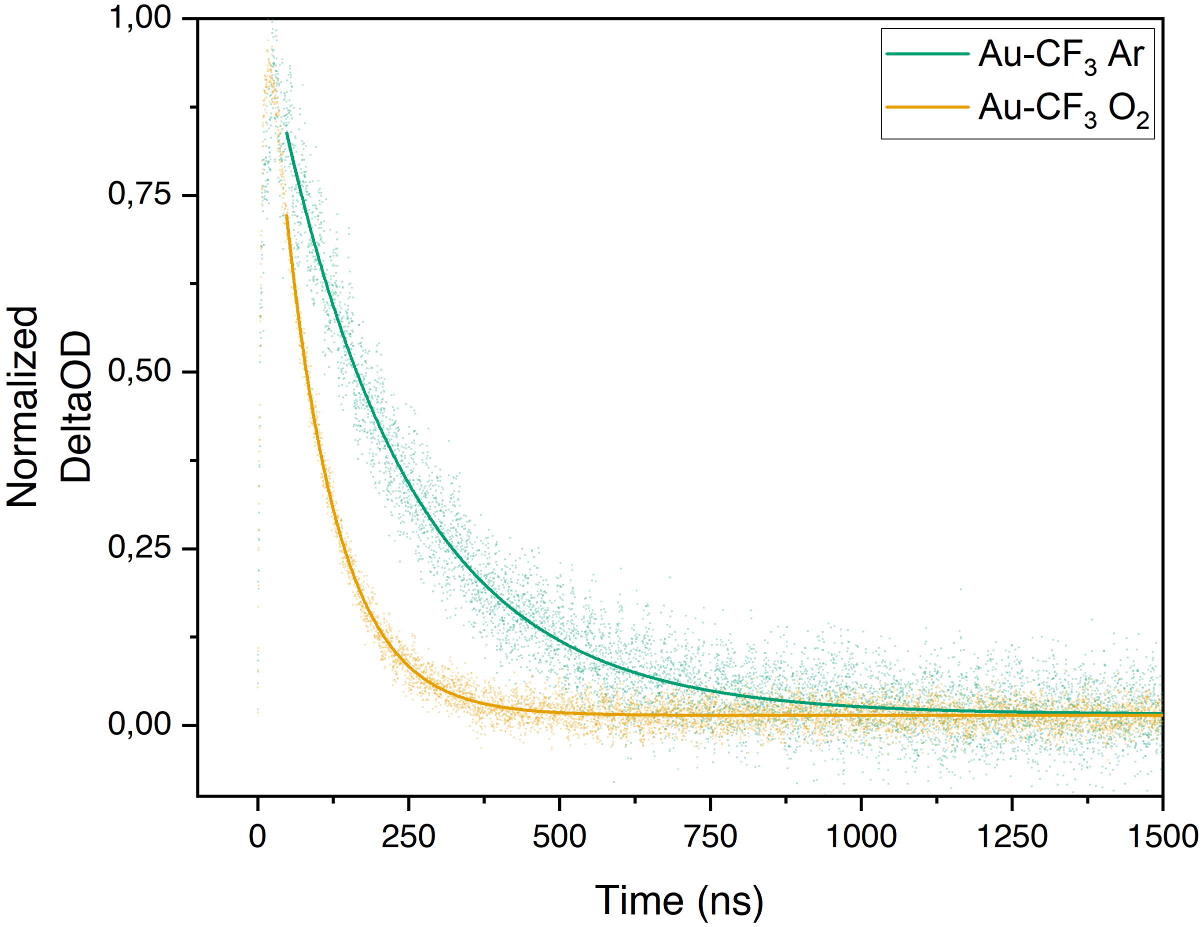

Fig. S7. Kinetic traces extracted at 400 nm, maximum of the TAS signal from Fig. S3, after excitation of the Au-CF$_3$ complex at 355 nm. The graph compares the signal decay in inert gas (Argon) and in the presence of oxygen.

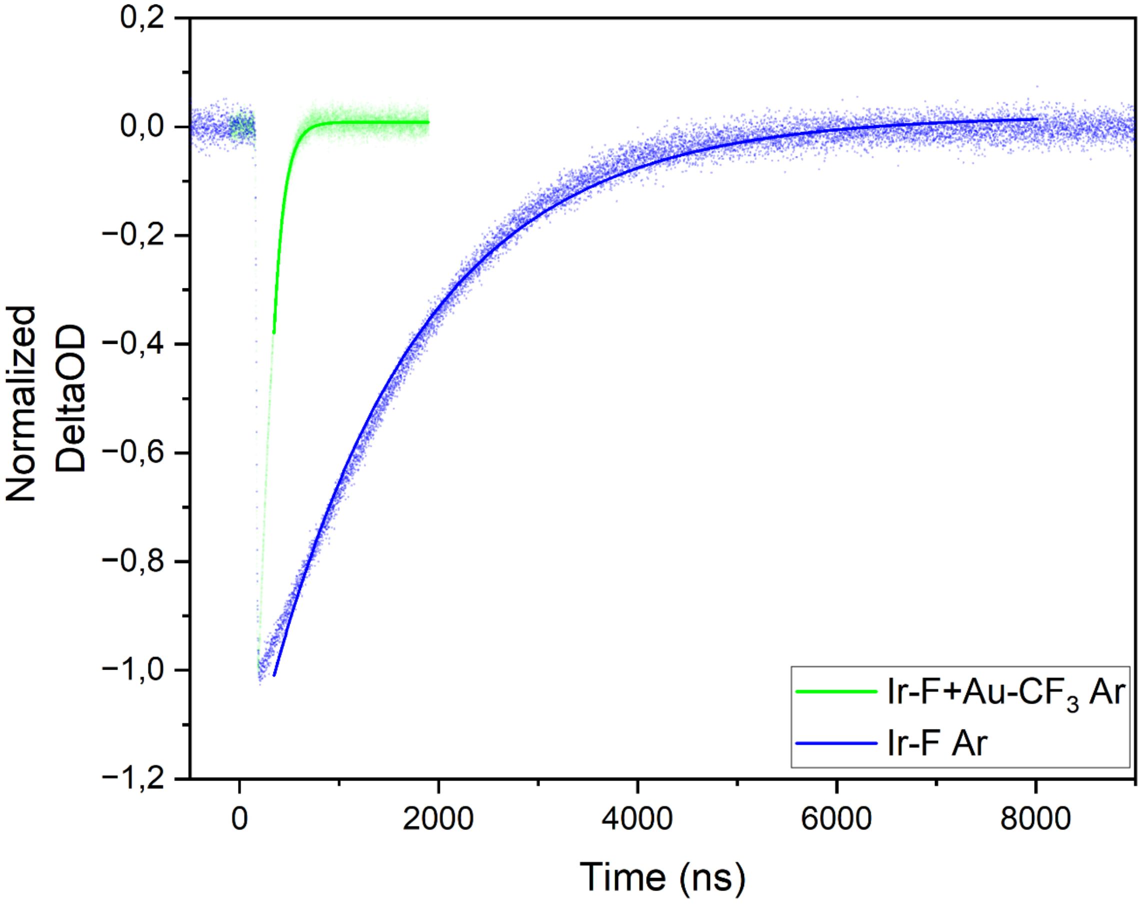

Fig. S8. Kinetic traces extracted at 490 nm, minimum of the TAS signal from Fig. S1 and 1a), after excitation of the Ir-F photosensitizer at 410 nm. The graph compares the signal decay in inert gas (Argon) when Au-CF_3 complex is added to the mixture.

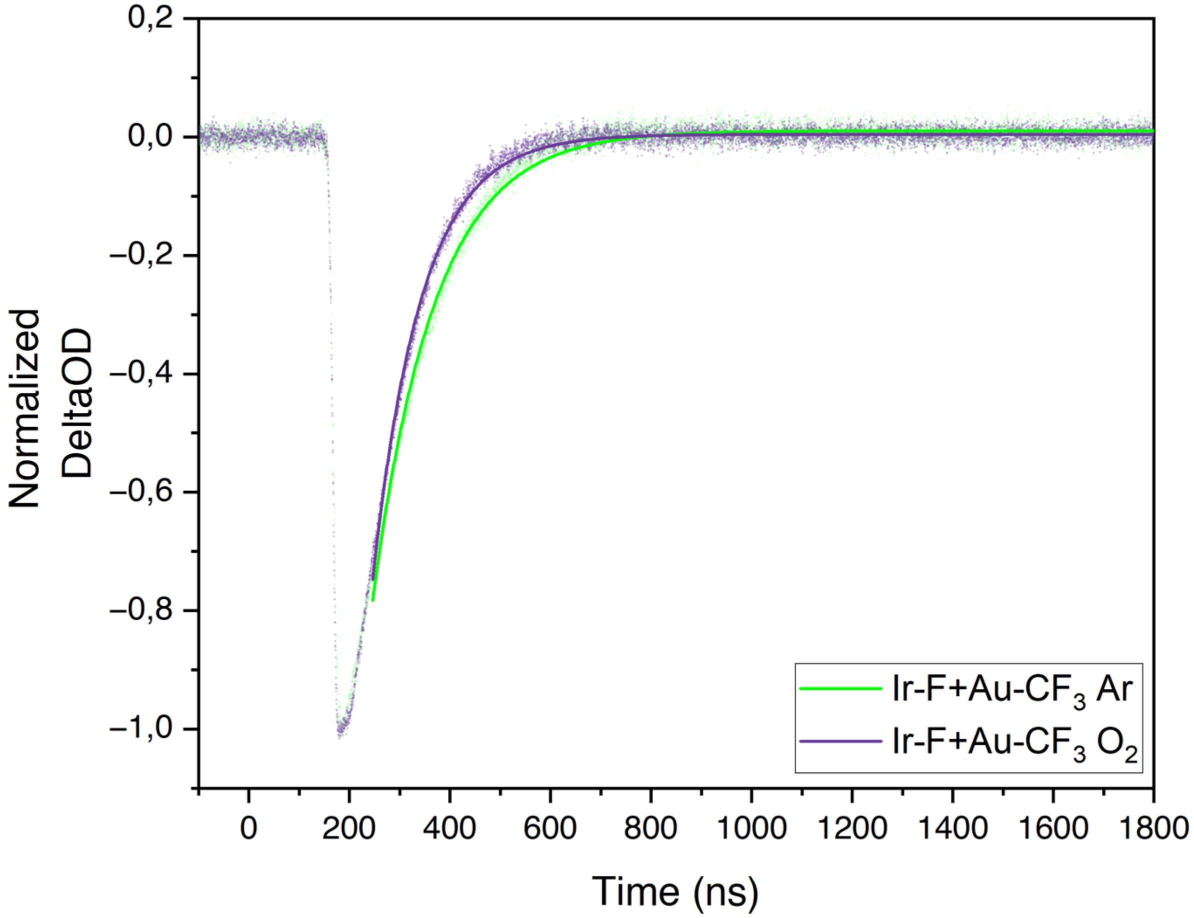

Fig. S9. Kinetic traces extracted at 490 nm after excitation of the Ir-F photosensitizer at 410 nm in the presence of Au-CF$_3$ complex. The graph compares the signal decay in inert gas (Argon) and in the presence of oxygen.

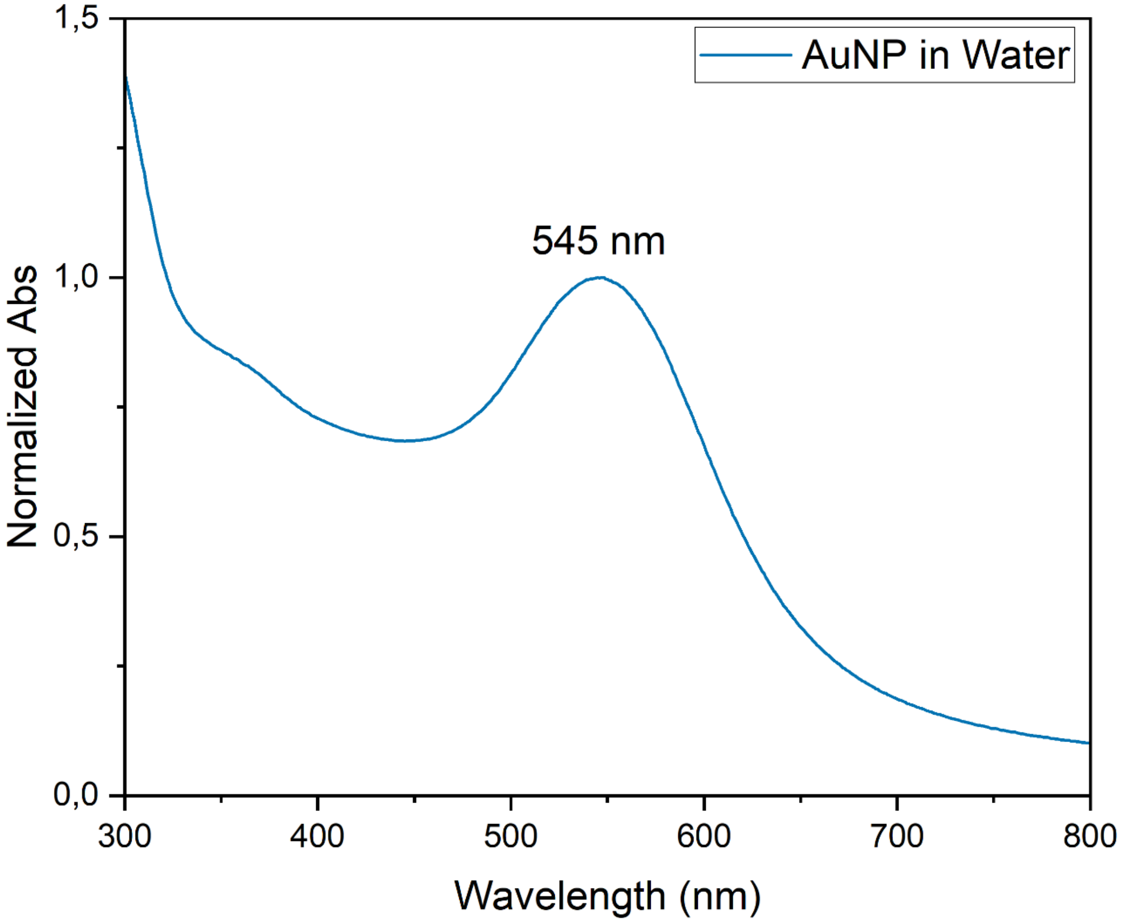

Fig. S10. UV-Vis of the AuNP in water.

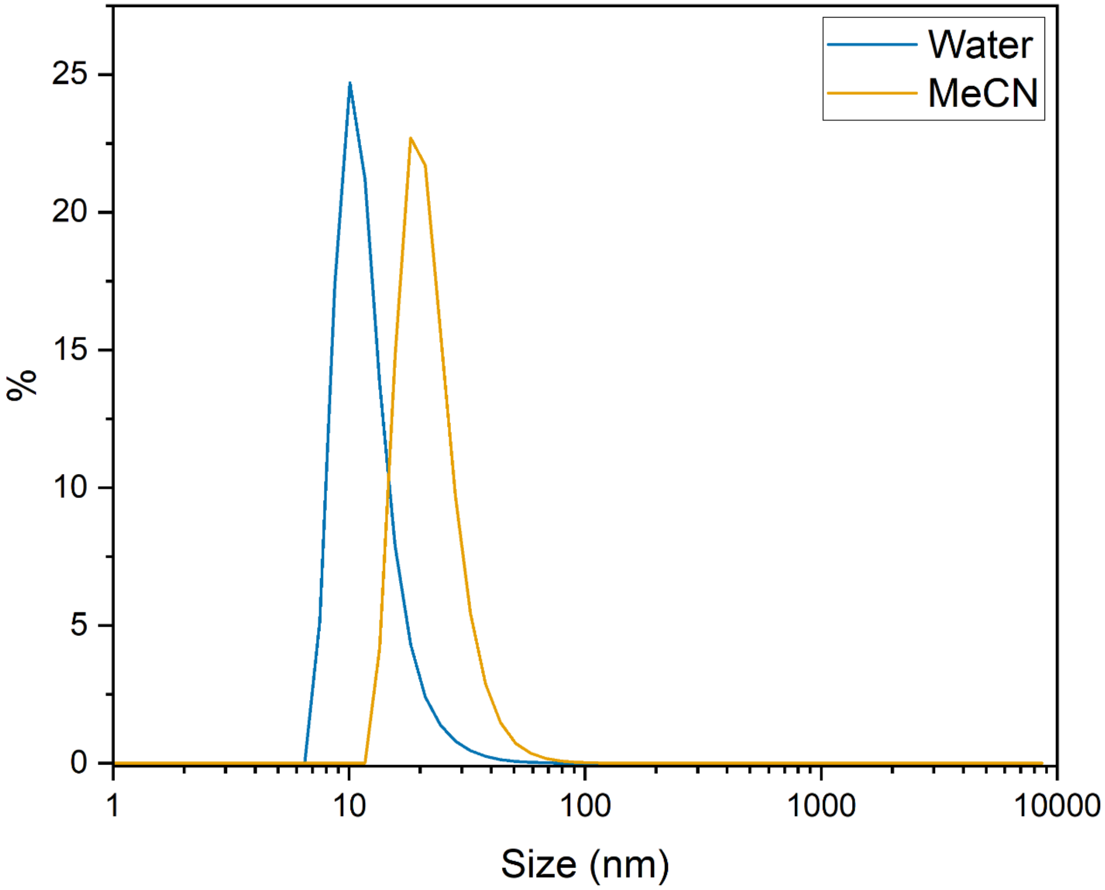

Fig. S11. Comparison of the DLS signal of AuNP in different solvents.

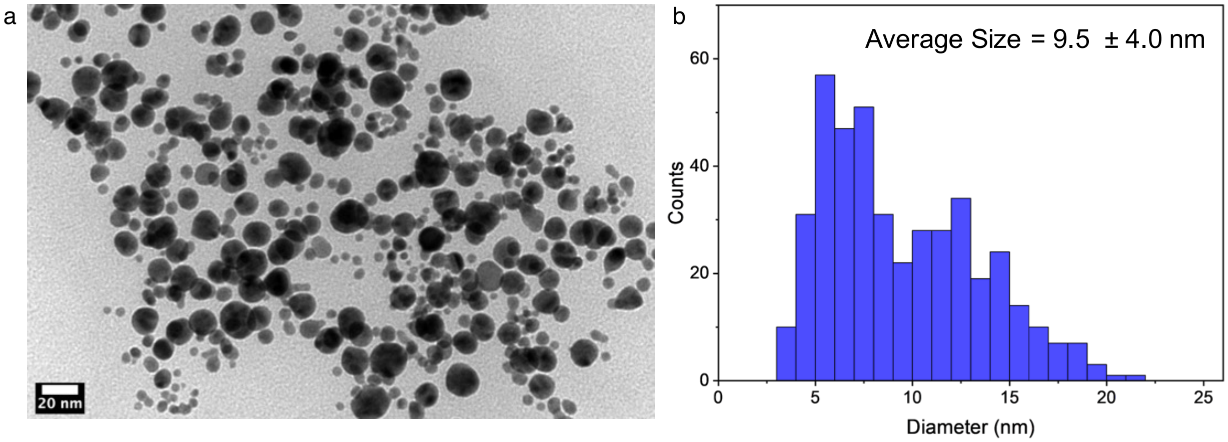

Fig. S12. TEM analysis of AuNP. a) TEM image of AuNP; and b) Histogram of the particles sizes.

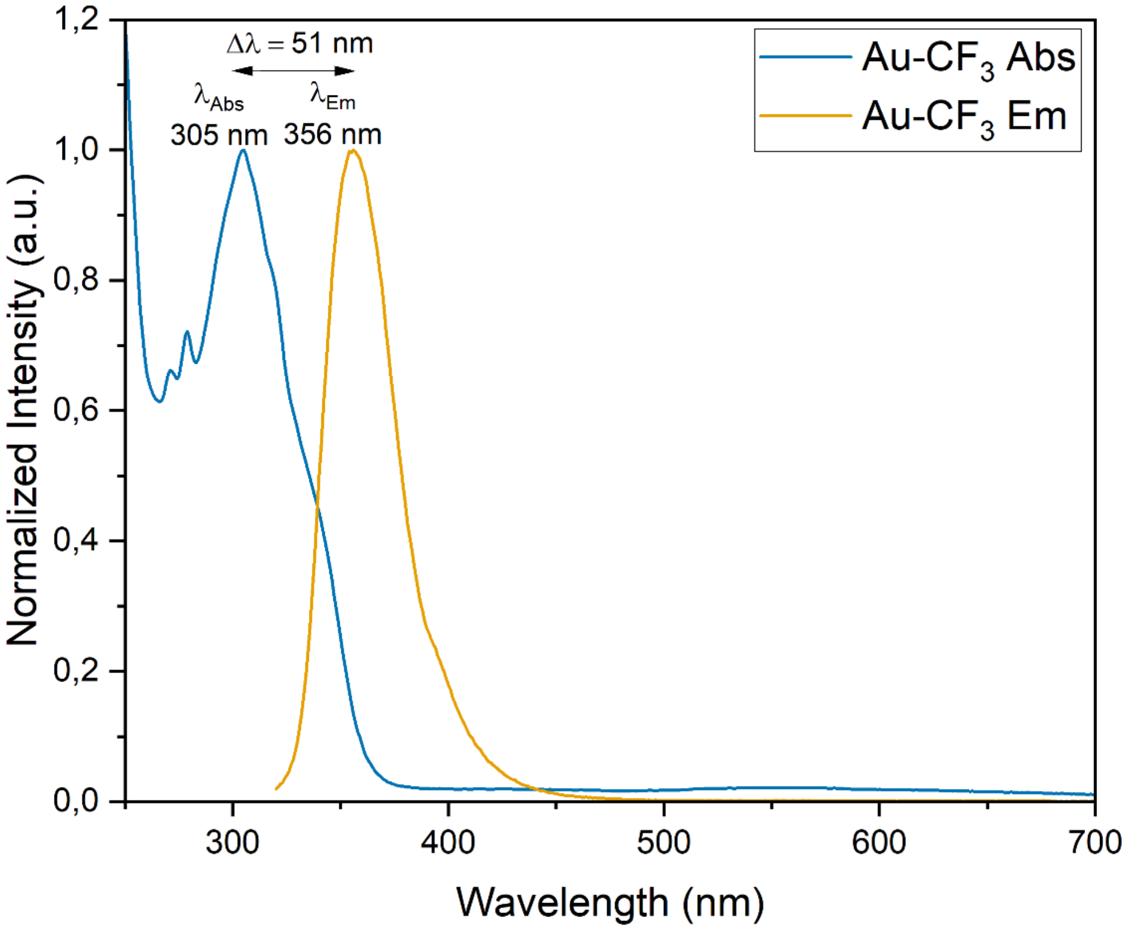

Fig. S13. Photoluminescence of Au-CF$_3$ in acetonitrile after excitation at 305 nm. The optical absorption of the complex is overlapped to evaluate fluorescence shift.

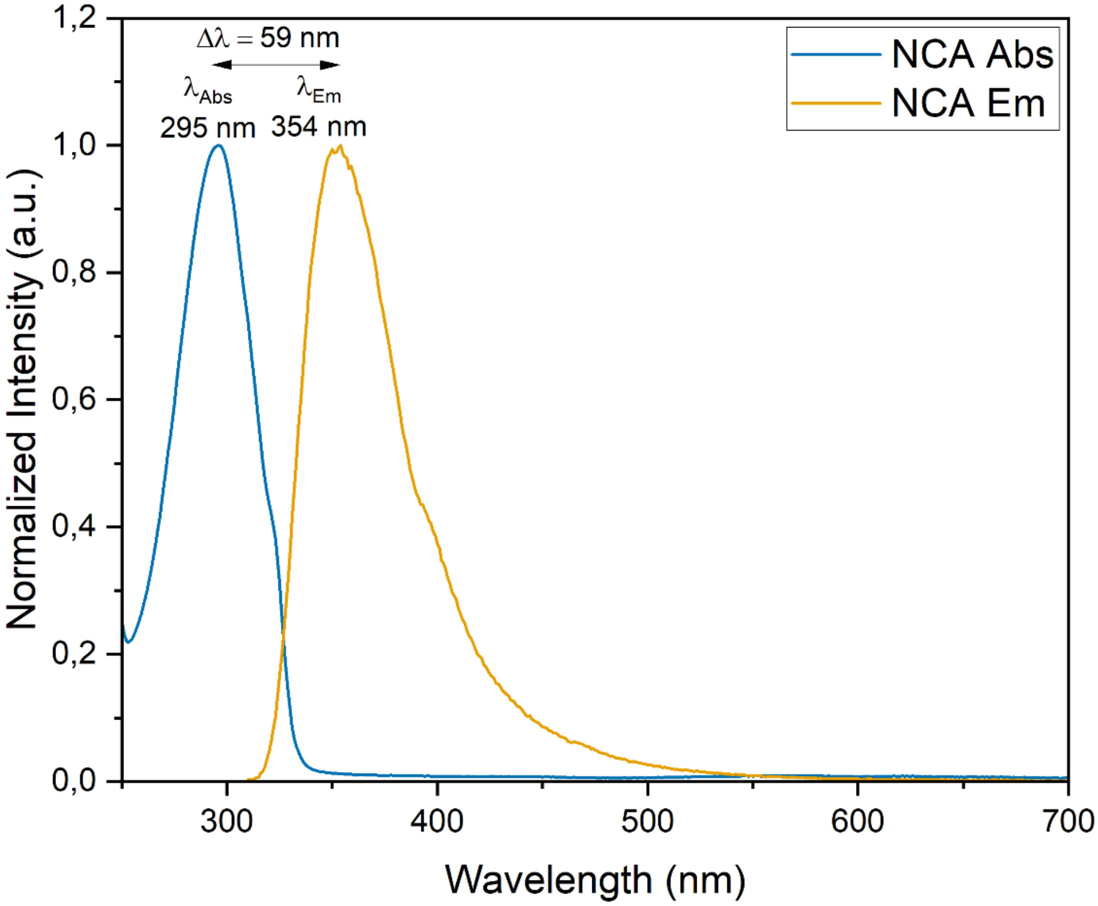

Fig. S14. Photoluminescence of NCA in acetonitrile after excitation at 295 nm. The optical absorption of the NCA is overlapped to evaluate fluorescence shift.

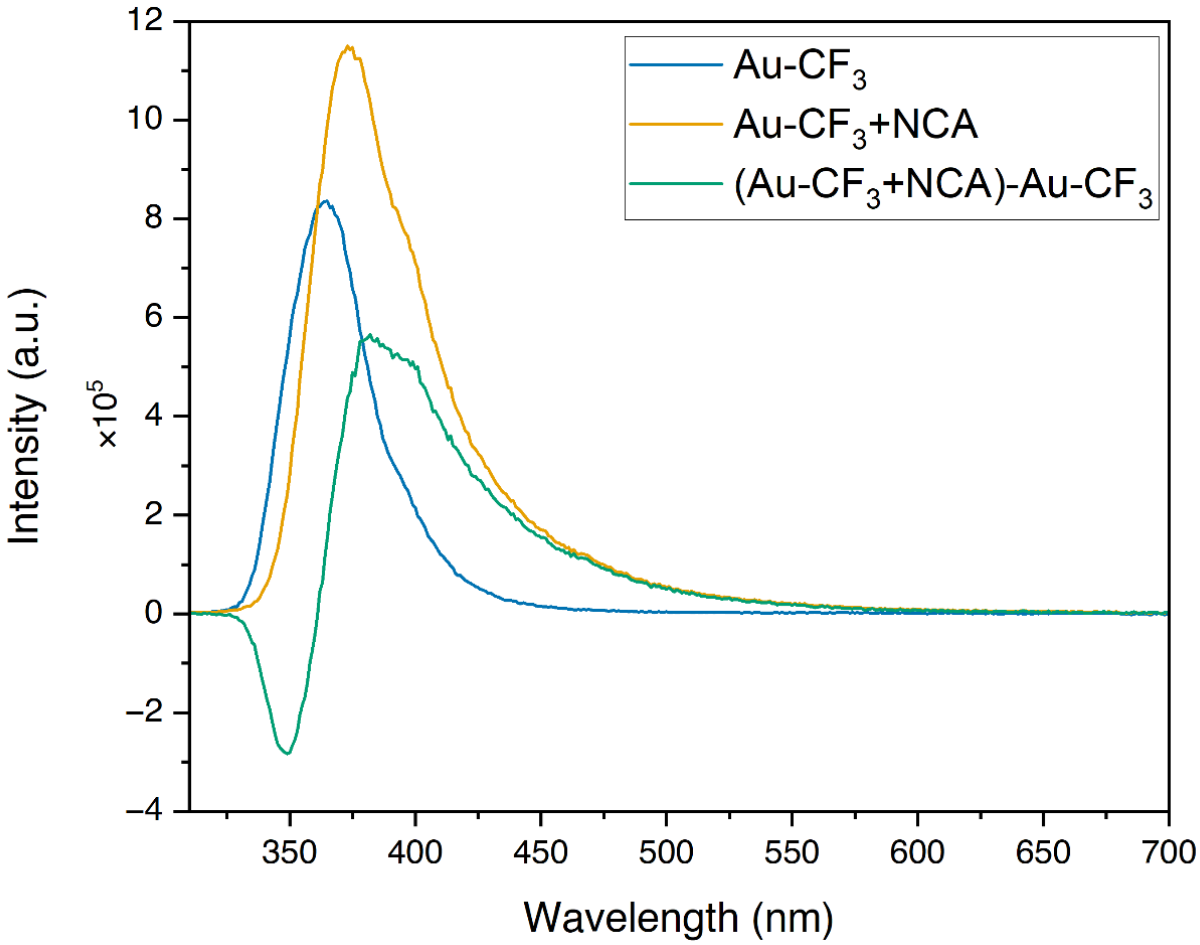

Fig. S15. Photoluminescence of Au-CF$_3$ and Au-CF$_3$ + NCA in acetonitrile after excitation at 295 nm.

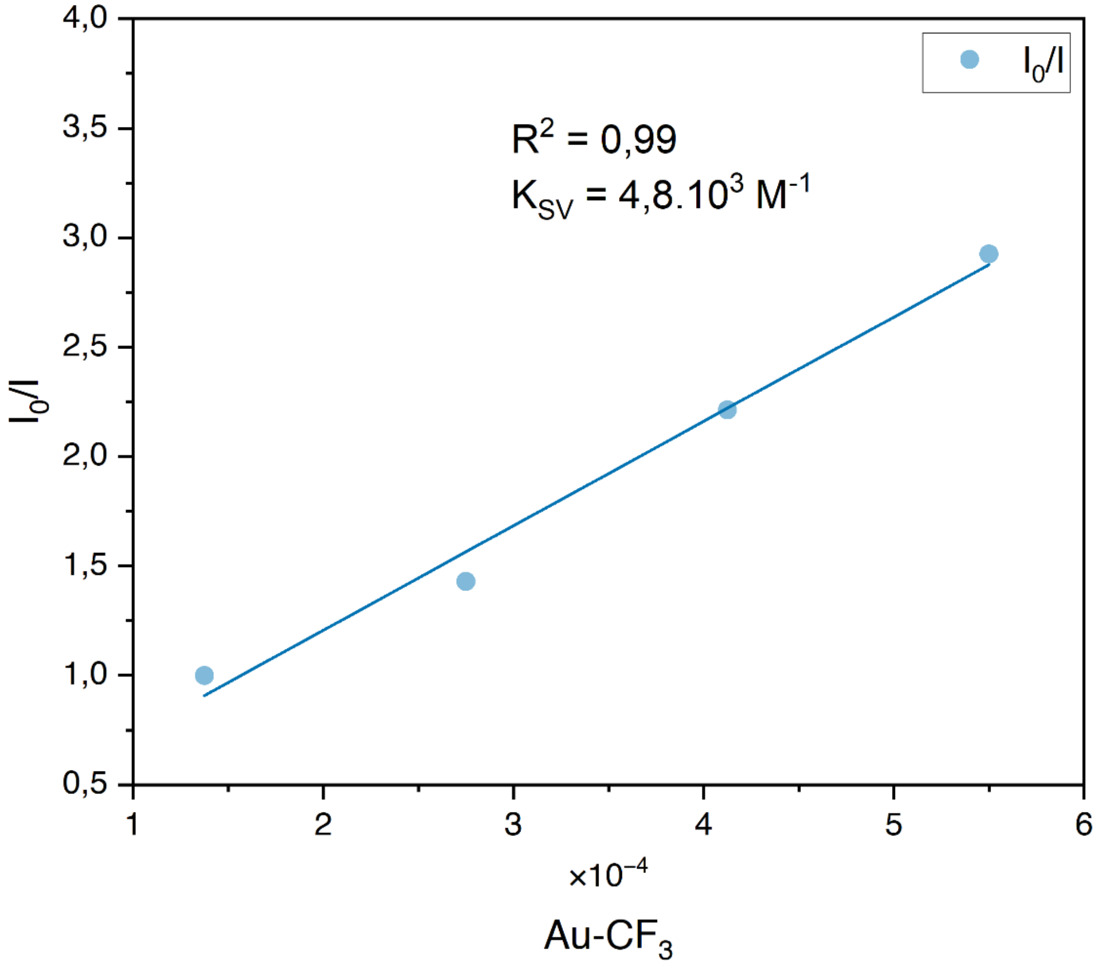

Fig. S16. Stern-Volmer plot of the fluorescence quenching of NCA in acetonitrile after excitation at 295 nm by Au-CF_3.

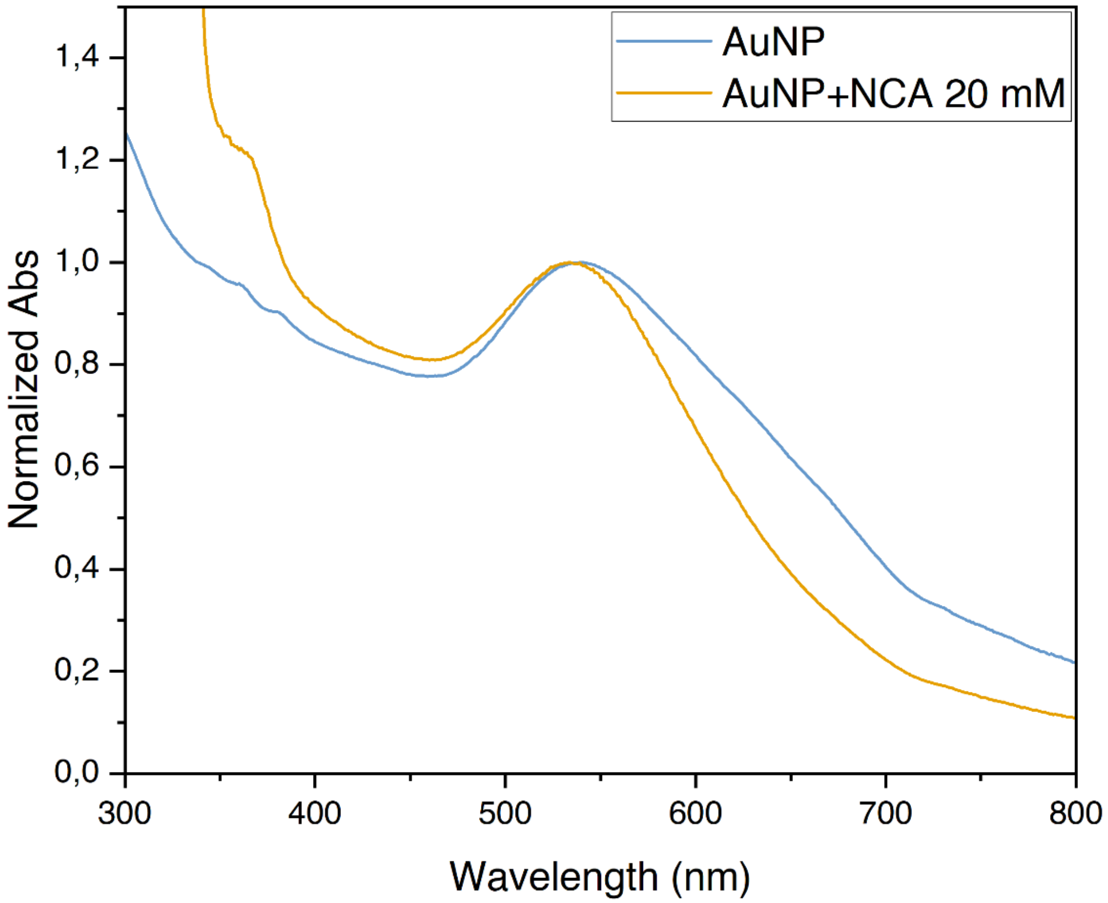

Fig. S17. Comparison of the UV-Vis of AuNP in acetonitrile after adding NCA.

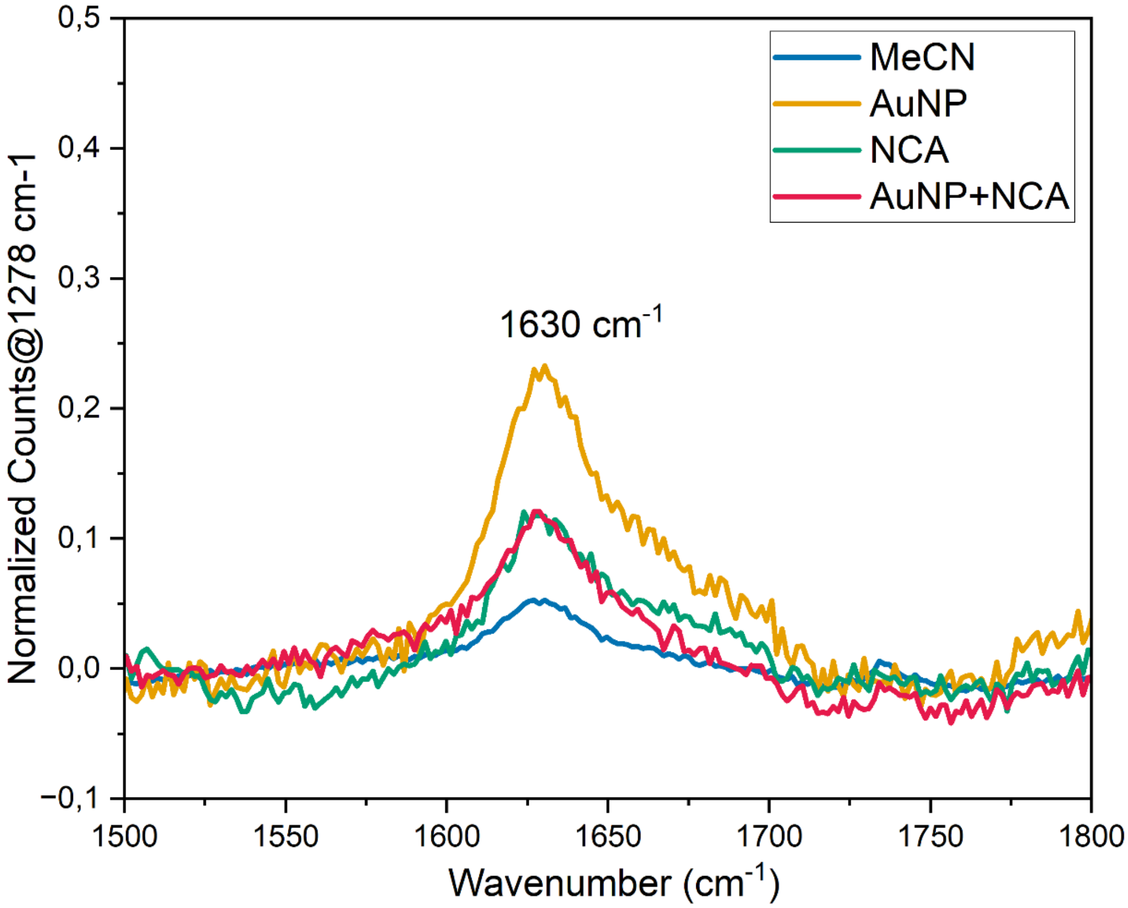

Fig. S18. Comparison of the Raman spectra in the carboxylic region.

References

---

1. a) Xia, Z. et al. Photosensitized Oxidative Addition to Gold(I) Enables Alkynylative Cyclization of o-Alkynylphenols with Iodoalkynes. *Nat. Chem.* **11**, 797–805 (2019); b) Zhao, F. et al. Reactant-induced photoactivation of in situ generated organogold intermediates leading to alkynylated indoles via C*sp*^{2}-C*sp* cross-coupling. *Nat Commun* **13**, 2295 (2022).

2. Piella, J. et al. Size-Controlled Synthesis of Sub-10-nanometer Citrate-Stabilized Gold Nanoparticles and Related Optical Properties. *Chem. Mater.* **28**, 1066–1075 (2016).

3. Han, X. et al. Role of salt in the spontaneous assembly of charged gold nanoparticles in ethanol. *Langmuir* **27**, 5282–5289 (2011).